LIMNOLOGY and OCEANOGRAPHY

ASLO

Limnol. Oceanogr. 71, 2026, e70285

doi: 10.1002/lno.70285

RESEARCH ARTICLE

Flow variability and macroinvertebrates jointly regulate stream periphyton and metabolism: Insights from experimental stream mesocosms

Flavia Tromboni,[1,2*] **Carolina Jativa**,[3] **Carina Seitz**,[4,5] **Alain Maasri**,[6] **Silvia Mohr**,[7] **Hans-Peter Grossart**,[8,9] **Giulia Grandi**,[10] **Enrico Bertuzzo**,[10] **Sonja C. Jähnig**,[2,11] **Clara Mendoza-Lera**,[1] **Andreas Lorke**,[1] **Marco Cantonati**,[12] **Anna Lupon**,[3] **Susana Bernal**[3]

[1]Institute for Environmental Sciences, University of Kaiserslautern-Landau (RPTU), Landau, Germany; [2]Department Community and Ecosystem Ecology, Leibniz Institute of Freshwater Ecology and Inland Fisheries (IGB), Berlin, Germany; [3]Integrative Freshwater Ecology Group, Centre d'Estudis Avançats de Blanes (CEAB-CSIC, Blanes, Spain; [4]Departamento de Geología y Petróleo, Centro Regional Universitario Bariloche, Universidad Nacional del Comahue-CONICET, San Carlos de Bariloche, Argentina; [5]Reno – Biology Department, and Global Water Center, University of Nevada, Reno, NV, USA; [6]Lower Saxony Water Management, Coastal Defense and Nature Conservation Agency (NLWKN), Hüde, Germany; [7]Division IV Chemical Safety, Section IV 2.5 Trace Analysis, Artificial Stream and Pond system, Berlin, Germany; [8]Department of Plankton and Microbial Ecology, Leibniz Institute of Freshwater Ecology and Inland Fisheries (IGB), Stechlin, Germany; [9]Institute of Biochemistry and Biology, Potsdam University, Potsdam, Germany; [10]Departmentof Environmental Sciences, Informatics and Statistics, University of Venice Ca' Foscari, Venice, Italy; [11]Geography Department, Humboldt-Universität zu Berlin, Berlin, Germany; [12]BIOMELab, Department of Biological, Geological and Environmental Sciences –BiGeA, Alma Mater Studiorum – University of Bologna, Bologna, Italy

Abstract

Climate change profoundly alters riverine flow regimes and community composition, affecting key ecosystem functions. We used an experimental mesocosm approach to examine how gradual flow velocity reduction (Experiment 1) and flushing events (Experiment 2) influence periphyton community composition and metabolism, with and without a macroinvertebrate assemblage. We prepared eight stream mesocosms with pre-grown periphyton, half including macroinvertebrates. Six mesocosms gradually transitioned from high (0.25 m s^{-1}) to low flow velocity (0.05 m s^{-1}), followed by three flushing events of increasing frequency (i.e., reducing time between events) and same intensity, raising from 0.05 to 0.25 m s^{-1} for 6 h before returning to base flow. Two control mesocosms (one with and one without macroinvertebrates) remained at constant flow (0.1 m s^{-1}) throughout the experiment. We measured algal biovolume, taxonomic composition, and metabolic rates (gross primary production; ecosystem respiration; net ecosystem production) over time. Macroinvertebrates altered community composition and reduced algal biovolume, with stronger effects at low flow. Flow reduction had scale-dependent effects: at the chamber scale it lowered periphyton gross primary production and net ecosystem production, while at the whole-mesocosm scale it decreased ecosystem respiration more than production, increasing net ecosystem production. Flushing events decreased algal biovolume, but enhanced periphyton autotrophy, though this effect weakened with repeated disturbance. Macroinvertebrate assemblages, while reducing total algal biovolume, enhanced the resistance of metabolic responses to flushing. Together, these results show that hydrological variability and macroinvertebrate presence jointly regulate periphyton structure and function and provide mechanistic insight into the processes controlling carbon cycling in running waters.

*Correspondence: flavia.tromboni@rptu.de

Associate editor: Robert O. Hall, Jr.

Freshwater ecosystems are experiencing rapid and pervasive transformations caused by ongoing climatic changes altering their hydrological regimes (IPCC 2022). The frequency and intensity of extreme oscillations between droughts and floods have been increasing, and biodiversity has dramatically declined (Maasri et al. 2022; Sayer et al. 2025). These changes can have critical consequences for stream functioning because river flow shapes fluvial communities' taxonomic and functional composition (Poff et al. 1997; Palmer and Ruhi 2019), and strongly influences fundamental ecosystem functions, including biogeochemical fluxes (Cunha et al. 2018; Tromboni et al. 2020) and organic matter turnover and storage (O'Donnell and Hotchkiss 2022). Flow velocity controls the deposition and resuspension of organic matter from the benthic sediments into the water column, influencing turbidity and limiting light penetration and photosynthesis (Kirk 1994; Uehlinger et al. 2000).

Variability in flow magnitude and frequency can influence biomass accumulation and the development of periphyton biofilm (i.e., bacteria, fungi, algae) (Uehlinger et al. 2003). In particular, an increase in the frequency of flow disturbances—that is, a shorter interval between spates—may favor generalists or r-selected species whose trait expression is adapted to disturbance, altering seasonal succession and shifting community composition by primarily selecting for generalist organisms (Shabarova et al. 2021; Stach et al. 2024). Given that periphyton and biofilm sediments dominate the metabolic activity in most streams (Battin et al. 2016; Tromboni et al. 2022), such changes can have large implications for critical ecosystem functions, especially carbon cycling and greenhouse gas emissions (Battin et al. 2023).

Flow variability controls variation in riverine metabolism (Bernhardt et al. 2022), gross primary production (GPP)—the synthesis of organic compounds from carbon dioxide—and ecosystem respiration (ER)—the breakdown of organic matter and release of carbon dioxide (Hall and Hotchkiss 2017) and their net balance. Typically, riverine productivity is high when flows are stable (Mulholland et al. 2001; Bernhardt et al. 2022), whereas extreme flow variations create unstable conditions that can reduce productivity through mechanisms such as scouring, habitat loss, reduced light penetration, and nutrient export, all of which disrupt periphyton colonization and community stability (Uehlinger 2006). Flow reductions can alter sediment transport regimes; even at low flows (LFs), sand may be mobilized as migrating ripples, which profoundly influence streambed microbial activity and thereby alter GPP and ER (Scheidweiler et al. 2021). GPP and ER can respond differently to changes in flow velocity and the frequency of extreme events, whereby various studies indicate that GPP is generally more sensitive to extreme environmental changes than ER (O'Donnell and Hotchkiss 2022). GPP can decline immediately after flood events due to the scouring and removal of periphyton, whereas ER tends to be more resistant, as heterotrophic respiration depends on more persistent organic matter sources (Uehlinger 2000). Additionally, GPP and ER can exhibit different recovery patterns after disturbances, reflecting varying levels of ecosystem resilience (Uehlinger 2000; Jativa et al. 2025).

Although stream organisms have evolved to cope with occasional high-flow disturbances, the increased frequency of extreme events predicted under climate change may exceed their adaptive capacity, leading to substantial shifts in community composition and associated metabolic rates (Sabater et al. 2023). However, the effects of increased frequency of extreme events (flushing events hereinafter) on riverine metabolism remain largely unknown, limiting our understanding of potential impacts of climate change on riverine carbon fluxes. In turn, grazing aquatic macroinvertebrates can also influence the dynamics of periphyton biomass and functioning (Moulton et al. 2015) both directly, through grazing and thus top-down control (Arsenault et al. 2022), and indirectly through bioturbation— the physical disturbance of periphyton and redistribution of organic material (Steinman et al. 1995).

Macroinvertebrate assemblages can reduce periphyton biomass, with the magnitude of the effect depending on consumer type, ecosystem context, and local environmental characteristics (Lamberti and Resh 1983; Hillebrand 2009). However, few studies have quantified how diverse macroinvertebrate communities—comprising grazers, shredders, collector-gatherers, and predators—regulate GPP and ER, limiting our understanding of the mechanisms by which consumers influence metabolic rates (Rüegg et al. 2021). Consequently, we still lack a clear picture of how simultaneous declines in aquatic macroinvertebrate abundance and changes in flow regimes will affect riverine metabolism across temporal scales.

In this study, we used a mesocosm approach to assess how (1) a gradual reduction in flow velocity and (2) the increase in flushing frequency impact periphyton structural characteristics and metabolism, and how these effects are modulated by the presence of macroinvertebrate assemblages. We expect gradual flow reduction to shift periphyton toward greater heterotrophic dominance, both by favoring bacteria and fungi over autotrophs (community composition change) and by reducing autotrophic production through light limitation and organic matter accumulation (lower GPP, higher ER, and more negative NEP). In contrast, we expect that increasing flushing frequency will more strongly affect periphyton by physically removing biomass and thereby reducing GPP. Additionally, we predict that macroinvertebrates' grazing will further lower total periphyton biomass through direct consumption, while promoting a more autotrophic community (higher GPP) by removing senescent material and enhancing light penetration in the periphyton.

Methods

Experimental design

We conducted two successive experiments in eight indoor recirculating stream mesocosms at the German Federal Environment Agency in Berlin-Marienfelde, Germany (German Federal Environment Agency's artificial stream system:

https://www.umweltbundesamt.de/en/topics/chemicals/chemical-research-at-uba/artificial-stream-pond-system#the-artificial-stream-and-pond-system-introduction). The mesocosms were designed as 38-m long channels made of glass-fiber reinforced polyester and equipped with screw pumps to generate different flow velocities (Supporting Information Fig. S1 and Table S1). The experimental design consisted of six mesocosms that underwent different variations in flow velocity (see below). Three of these mesocosms contained pre-grown periphyton with a macroinvertebrate assemblage (hereafter, treatment "macroinvertebrates"), while the other three mesocosms only had pre-grown periphyton (hereafter, treatment "no macroinvertebrates"). The other two mesocosms (one with and one without macroinvertebrates) were controls that we maintained at a constant flow velocity throughout the experiment (Supporting Information Fig. S2). We randomly assigned mesocosms to each treatment group.

Experiment 1: Flow velocity reduction—This experiment assessed how periphyton characteristics responded to gradual changes in flow velocity. We maintained three mesocosms with macroinvertebrates and three without at high flow (HF) velocity (0.25 m s^{-1}) for 7 d starting on April 27, 2021. We then decreased the flow in two steps: first from 0.25 to 0.1 m s^{-1} and maintained it for 7 d as a transition phase and finally decreased it to 0.05 m s^{-1} for another 7 days (until May 18, 2021). We maintained the two control mesocosms at a constant flow velocity of 0.1 m s^{-1} throughout the experiment (Fig. 1).

Experiment 2: Flushing Events—Following the flow velocity reduction experiment, we subjected the six mesocosms to three flushing events of increasing frequency (From May 18 to May 27, 2021). During these events, flow velocity was abruptly increased from 0.05 to 0.25 m s^{-1} for 6 h before returning to base flow. The frequency of these flushing events progressively shortened from 240 h, 168 h, and finally to 18 h between flushes (Fig. 1). The two control mesocosms remained at a constant flow velocity of 0.1 m s^{-1} throughout experiment 2.

Sampling for periphyton characteristics occurred three times during HF, and three times during LF. The LF condition then served as the initial condition for experiment two, where periphyton was sampled after flushing event 1, 2, and 3 (Fig. 1, and see details further below in the methods).

Mesocosm configuration

We filled each mesocosm with 20 cm of pre-treated commercial sand as substrate and 20 cm of water. The sand substrate was chosen to resemble the natural benthic environment of a reference stream, the Lieberoser Mühlenfließ stream, Brandenburg, Germany, a sand bottom stream representative of most streams surrounding the mesocosm facility. The water temperature followed ambient conditions (March–May, 2021) inside the mesocosm hall. We maintained constant light conditions throughout the experiment with fluorescent tubes (OSRAM LF72) providing a 14:10 h light–dark cycle to simulate a shaded stream environment. The average light intensity was 3000 lx ($\sim$ 60 µE m^{-2} s^{-1}). To establish periphyton communities, we collected diatom-dominated periphyton from an outdoor pond at the German Federal Environment Agency field station. The periphyton was homogenized, and aliquots were evenly distributed across all mesocosms, with each mesocosm containing 18 tiles (made of the same material as the mesocosm walls) to allow for periphyton sampling over time. We allowed colonization to occur for 4 weeks under no-flow conditions before the start of the flow velocity experiments.

After 2 weeks of periphyton colonization, we stocked four of the mesocosms with a natural macroinvertebrate assemblage and kept them for the remaining 2 weeks of the total 4 weeks of periphyton colonization. We collected the macroinvertebrate community by means of 35 straw bags previously placed in the Lieberoser Mühlenfließ stream for 2 weeks, allowing colonization by the natural macroinvertebrate community. We used straw bags in a sand-bottom stream to collect a diverse macroinvertebrate community. The bags served primarily as a stable substrate that allowed colonization by multiple functional groups—including grazers, shredders, collector-gatherers, and predators—as documented in Table S2. We transferred eight bags into four mesocosms where periphyton had been growing for 2 weeks (Supporting Information Fig. S1). We used the other three bags to characterize the macroinvertebrate community transferred into the mesocosms (Supporting Information Table S2).

Macroinvertebrates characterization

We identified macroinvertebrates to the lowest taxonomic level under a dissection microscope (10×) according to Tachet et al. (2010). Macroinvertebrate communities were composed primarily of Amphipoda (*Gammarus* spp.) and insects. In total, 24 taxa were identified with the highest abundances for chironomids, followed by *Gammarus* spp. (Table S2). To monitor the growth of *Gammarus* over time, we selected groups of 10 individuals of *Gammarus* spp. and placed them in small cages partially filled with straw and ceramic beads, previously colonized by the same periphyton from the mesocosms. At the start of the experiment, we weighed four groups of 10 individuals of these *Gammarus* spp. to establish a baseline. Each week, we collected one cage per mesocosm to measure the increase in biomass of *Gammarus* spp. over time (AFDM) (Supporting Information Fig. S3). We used *Gammarus* spp. because they represented the highest biomass in the sampled natural community and were relatively easy to manipulate.

Periphyton biovolume and taxonomic characterization of the algal component

We assessed periphyton biovolume and taxonomic composition by collecting a tile at every sampling time. We scrubbed the entire material of the tile and preserved the samples in Lugol's solution (APHA 2012). For taxonomic characterization, we only used samples from May 3, May 17, and May 24 (Fig. 1). Samples after flushing events 2 and 3 were not well preserved and we could not use them for identification.

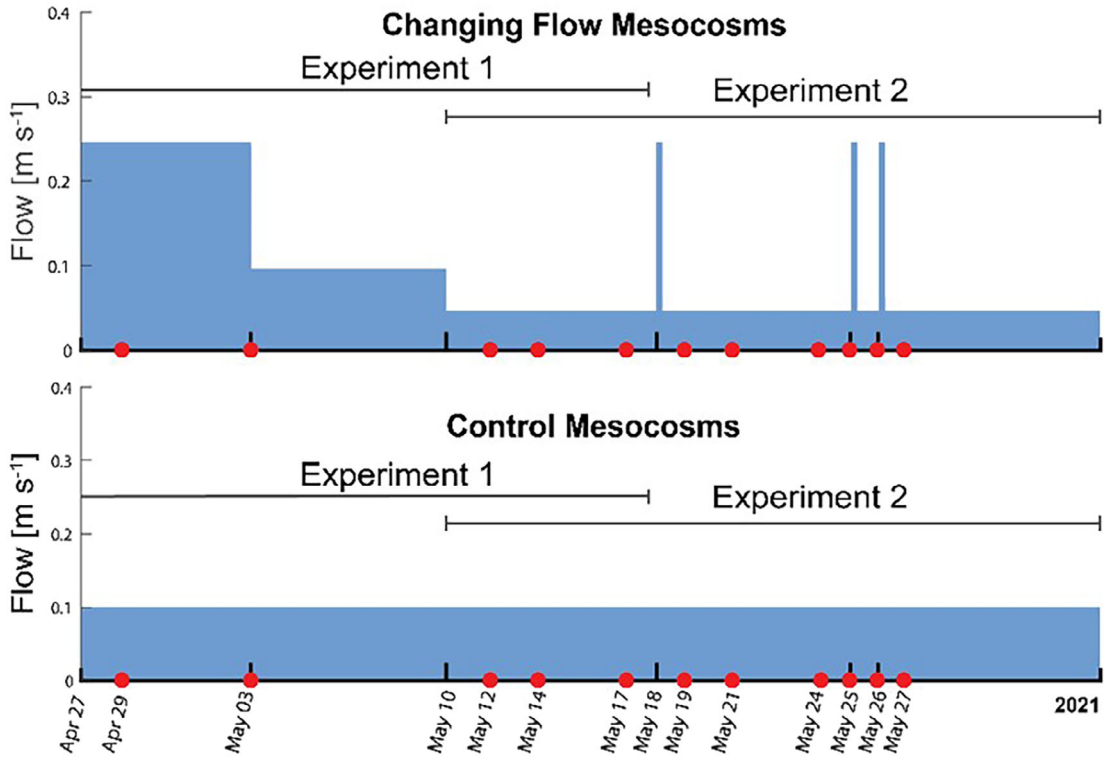

Fig. 1. Scheme of the experimental design. Experiment 1—flow velocity reduction (April 27–May 17, 2021): six mesocosms with flow velocity initially set at 0.25 m s^{-1}, then reduced to 0.1 m s^{-1} for a 7-d transition before reaching 0.05 m s^{-1} for another 7-day period. Experiment 2—flushing events (May 18–May 27, 2021): six mesocosms underwent three flushing events of increasing frequency, where flow was abruptly increased from 0.05 to 0.25 m s^{-1} for 6 h before returning to base flow. Two mesocosms (control) were maintained at a constant flow velocity of 0.1 m s^{-1} throughout both experiments. Red dots represent periphyton sampling dates.

We analyzed algal taxonomic composition under a microscope following standard counting protocols. After homogenization, we placed a 0.113 mL subsample into a Palmer-Maloney counting cell (Palmer and Maloney 1954) and examined it under a microscope at 400× magnification. We assessed the algal community composition by counting at least 300 algal units, including diatoms with plastids, using natural counting units as defined by Noble et al. (2023). Algal unit density per field of view was verified before counting to ensure accurate identification.

We used a Zeiss compound microscope with a digital camera and TopView software for taxonomic identification. We prepared water mounts for photomicrographs and algal unit descriptions. We measured algal units, photographed, assigned taxonomic names, and identified them to the lowest possible taxonomic level. Identification resources included the Diatoms of North America website (Serieyssol 2012; Bellinger and Sigee 2015; Weehr et al. 2015; Spaulding et al. 2021); and the species nomenclature was verified using Guiry and Guiry (2023). We converted algal counts to biovolume per surface area (μm^3 cm^{-2}), following the approach of Rimet and Druart (2018) and using average cell dimensions from at least 10 cells per taxon to estimate biovolume. The relative abundance of the dominant four diatom species (present in 80% of the samples) was explored in relation to flow conditions and the presence of a macroinvertebrate assemblage.

Metabolism measurements

We assessed metabolism at two different spatial scales: chamber vs. whole-mesocosm metabolism. (1) *Chamber metabolism*—At each sampling date (three times during HF, LF, and the first flushing event, one time after the increase in frequency flushing events 2 and 3) (Fig. 1), we used sealed recirculating chambers to incubate individual tiles to estimate only periphyton-specific metabolism, following the protocols of Tromboni et al. (2017); and Tromboni et al. (2020). We used chambers constructed from plexiglass with a propeller-driven helice to create a laminar flow (same described by Rüegg et al. 2015). Although the flow velocity in the chambers was lower than in the mesocosms, we standardized it across all chamber incubations to ensure consistent metabolic estimates. Chambers were equipped with dissolved oxygen (DO) and temperature YSI ProODO optical sensors (Yellow Springs Instruments, Yellow Springs, Ohio, USA) measuring every minute. We conducted both light incubations and dark incubations by covering the chambers with dark

plastic. Each incubation was kept for 1 h. (2) *Whole-mesocosm metabolism*—This method accounted for whole system metabolism, including contributions from periphyton, water column with suspended organic matter, and sediment respiration. We deployed DO and temperature sensors (FDO701 IQ and Sensotyt700 IQ, WTW, Germany) in the mesocosms during the entire experiment, recording hourly measurements.

Metabolism estimates

Chamber metabolism

Metabolic rates (GPP, ER, and NEP) were determined by linear regression of DO changes over time, both in the dark (for ER) and under light (for NEP), as follows (Eq. 1):

$$\text{Metabolic Rate} = \frac{\Delta O_2 \cdot V}{A} \quad (1)$$

where ΔO_2 (mg L^{-1}) is the rate of change in oxygen over time and is represented by the slope of the regression; V is the volume of the chamber; and A is the area of the tile with periphyton.

We then determined GPP from NEP and ER as (Eq. 2):

$$\text{GPP} = \text{ER} + \text{NEP} \quad (2)$$

Whole-mesocosm metabolism

We estimated total metabolism in the mesocosms (whole-mesocosm metabolism) with daily resolution during each experiment using the open-channel method (Odum 1956). The observed DO concentration $[O_2]$ at each sampling time t was used to establish the following mass balance (Eq. 3):

$$\frac{d[O_2]}{dt} = \left(\text{GPP}_i \cdot \frac{\text{RAD}(t)}{\langle \text{RAD}_i \rangle} + \text{ER}_i\right)\frac{1}{z} + K_{O_2}\left([O_2]_{sat}(t) - [O_2](t)\right)$$

where $[O_2]_{sat}$ (mg L^{-1}) is the 100% DO saturation concentration at time t calculated using eq. 18 from Grace and Imberger (2006), GPP_i and ER_i (g m^{-2} d^{-1}) represent each of these metabolic rates for day i, respectively, K_{O_2} is the oxygen exchange rate at time t, RAD is the radiation normalized to its daily mean value $\langle RAD \rangle_i$ and z is water depth.

For each experimental day, we estimated GPP and ER as model parameters by solving differential Eq. 1 in the MATLAB® environment using the DreamZS Bayesian framework (ter Braak and Vrugt 2008). Although data were collected at 1-h intervals, we discretized Eq. 1 into 10-min modeling steps and solved it using a forward Euler scheme. We assumed minimally informative uniform prior distributions (within the limits shown in Supporting Information Table S3) and independent, identically distributed normal observation errors with standard deviation $\sigma\epsilon$. Further information about the model parameters and K_{600} estimation is provided in the Supporting Information, section "Metabolism Modelling: Parameter Estimation."

Statistical analyses

We used the mesocosm as the experimental unit ($n = 3$ per treatment) and averaged subsamples within mesocosms (e.g., tiles, chambers, or repeated measurements) to obtain technical replicates. We included the two control mesocosms ($n = 1$ each, with and without macroinvertebrates) for descriptive comparison but excluded them from inferential statistics. We analyzed metabolic rates as response variables (GPP; ER; and NEP) with linear mixed-effects models of the form: Response ~ Flow × Macro + (1|Mesocosm). Flow treatment and Macro (macroinvertebrates present/absent) were treated as fixed factors and Mesocosm as a random intercept. NEP and ER were transformed using the inverse hyperbolic sine (asinh), which preserves the sign of negative values, and GPP was transformed using the natural log of one plus the value (log1p) to account for zeros and skew. From these models, we extracted estimated marginal means (emmeans), back-transformed them to the original scale, and reported them with 95% confidence intervals (CIs). We used LF as the reference condition and computed pairwise contrasts to test how metabolic rates under flushing events (F1–F3) or HF differed from LF, separately for mesocosms with and without macroinvertebrates. These contrasts were performed on the transformed model scale, and p values were adjusted for multiple comparisons using the Holm method to control the family-wise error rate. Thus, we specifically tested whether GPP, ER, and NEP under each treatment (e.g., HF vs. LF, F1 vs. LF, F2 vs. LF, F3 vs. LF) differed significantly from the LF baseline within each macroinvertebrate condition. Figures display raw mesocosm values together with back-transformed model estimates ± 95% CI. We report Holm-adjusted p values ($\alpha = 0.05$) but interpret them cautiously given the limited replication ($n = 3$). Our emphasis is on effect sizes and confidence intervals, and we avoid equating non-significant results with evidence for no effect. Analyses were performed in R (R Core Team 2022).

Results

Macroinvertebrate growth

Biomass of *Gammarus* spp. increased steadily throughout the experiment, particularly after the first week (T1), confirming that the caged individuals persisted and grew in the mesocosms. Average AFDM nearly doubled from acclimation (T1) to the end of the experiment (T5), demonstrating that macroinvertebrate biomass was maintained and increasing, thereby ensuring a consistent top-down

pressure during the experiment (Supporting Information Fig. S3).

Periphyton biovolume and diversity

Flow reduction

The presence of macroinvertebrate assemblage reduced algal biovolume under both HF and LF treatments. Further, the effect of flow velocity on algal biovolume depended on the presence of macroinvertebrates: in the absence of macroinvertebrates, algal biovolume did not change with decreasing flow velocity, whereas it decreased by 70% when macroinvertebrates were present (Fig. 2a).

Macroinvertebrates also altered periphyton taxonomic composition, particularly at the algal-group level. Across all mesocosms, Bacillariophyta were predominant, but in the absence of macroinvertebrates under LF conditions, Zygnematales increased markedly (+89.1%) and Cyanobacteria decreased (−61.7%), producing a shift from Cyanobacteria dominance at HF to Chlorophyta at LF (Fig. 2a).

Within Bacillariophyta (the dominant algal group), species-level compositional changes across treatments were comparatively modest (Fig. 2b). In control mesocosms with macroinvertebrates, *Achnanthidium minutissimum* and *Fragilaria crotonensis* prevailed, representing 32% and 35% of the total Bacillariophyta population, respectively. *Diatoma tenuis* predominated without macroinvertebrates and under reduced flow velocity. These four Bacillariophyta taxa accounted for most of the Bacillariophyta community, and their relative contributions explain the patterns illustrated in Fig. 2b.

Flushing events

Algal biovolume was consistently lower in mesocosms with macroinvertebrates than in those without, across all

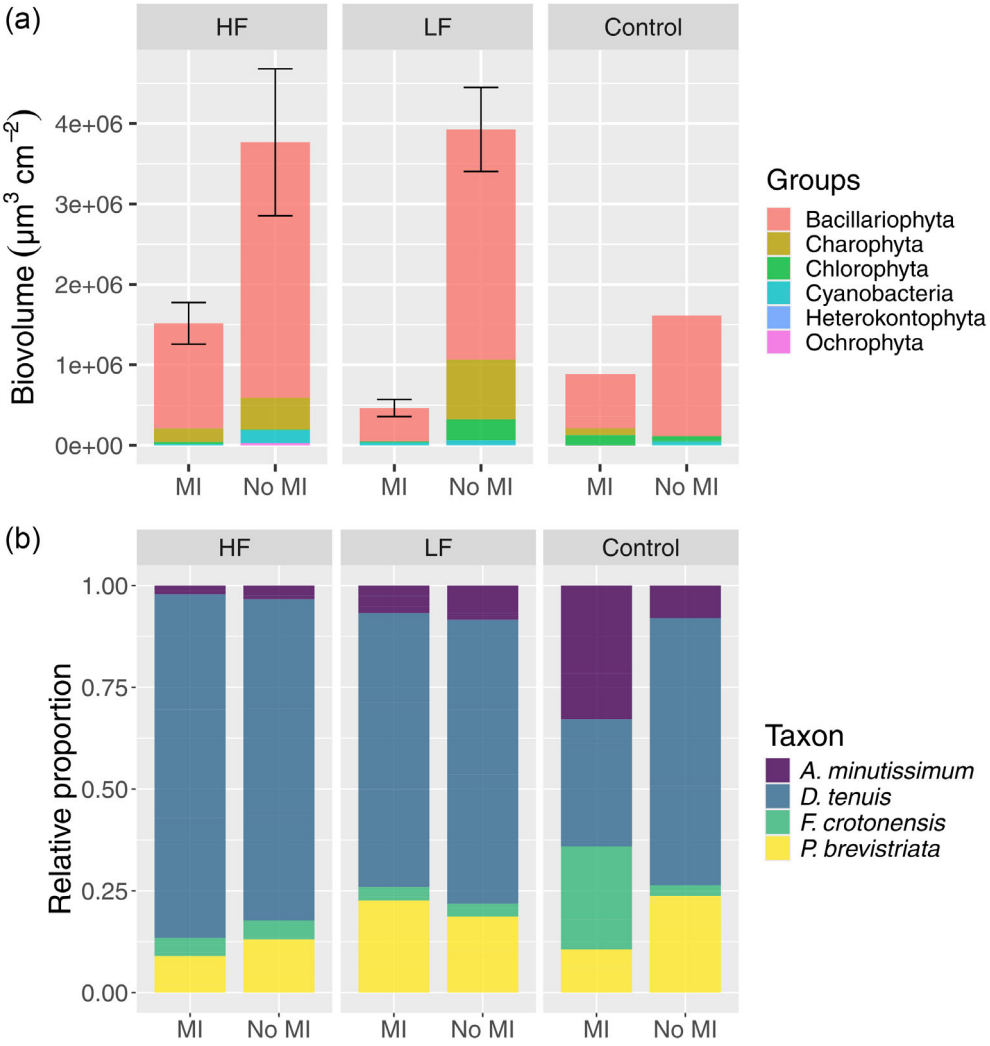

Fig. 2. (**a**) Mean biovolume of different algal groups (error bars represent standard error among mesocosms, $n = 3$ per treatment) and (**b**) relative proportions of the four dominant Bacillariophyta taxa, expressed as percentages of total Bacillariophyta biovolume, at high flow (HF) and low flow (LF), with macroinvertebrates (MI) and without macroinvertebrates (No MI). Control mesocosms ($n = 1$ each) are shown for descriptive purposes only.

treatments. In both cases, total algal biovolume decreased after the first flushing event by 24% and 38% in the mesocosms with and without macroinvertebrates, respectively (Fig. 3a). The periphyton taxonomic composition differed between mesocosms with and without macroinvertebrates (Fig. 3b). Bacillariophyta dominated the community under all flow conditions, but the relative proportions among the four dominant Bacillariophyta taxa shifted in the presence of macroinvertebrates (Fig. 3b): *A. minutissimum* became proportionally more dominant, whereas *D. tenuis* declined (−51% and −10% in the F1 and Control treatments, respectively). In addition, at the group level, the proportion of Zygnematales (mostly *Mougeotia* spp.) decreased significantly in experiments without macroinvertebrates following the flushing event (Fig. 3a). Since all Charophyte taxa identified in our samples belong to the genus *Mougeotia*, we classified them under the order Zygnematales rather than the broader phylum Charophyta, to avoid potential confusion with stoneworts (true charophytes).

Metabolism

Flow reduction

Reduced flow lowered autotrophy in chambers but dampened heterotrophy in mesocosms, with flow regime exerting a stronger influence than macroinvertebrate presence. GPP and ER estimates revealed both similarities and contrasts between chamber-based and whole-mesocosm methods. The presence of macroinvertebrates had only minor effects on GPP and ER, with no consistent differences between treatments. At the chamber scale, the periphyton remained autotrophic under both HF and LF conditions (GPP > |ER|), although productivity declined markedly at LF (Fig. 4a). In contrast, at the whole-mesocosm scale, HF mesocosms were strongly heterotrophic (|ER| ≫ GPP), whereas LF mesocosms shifted closer to

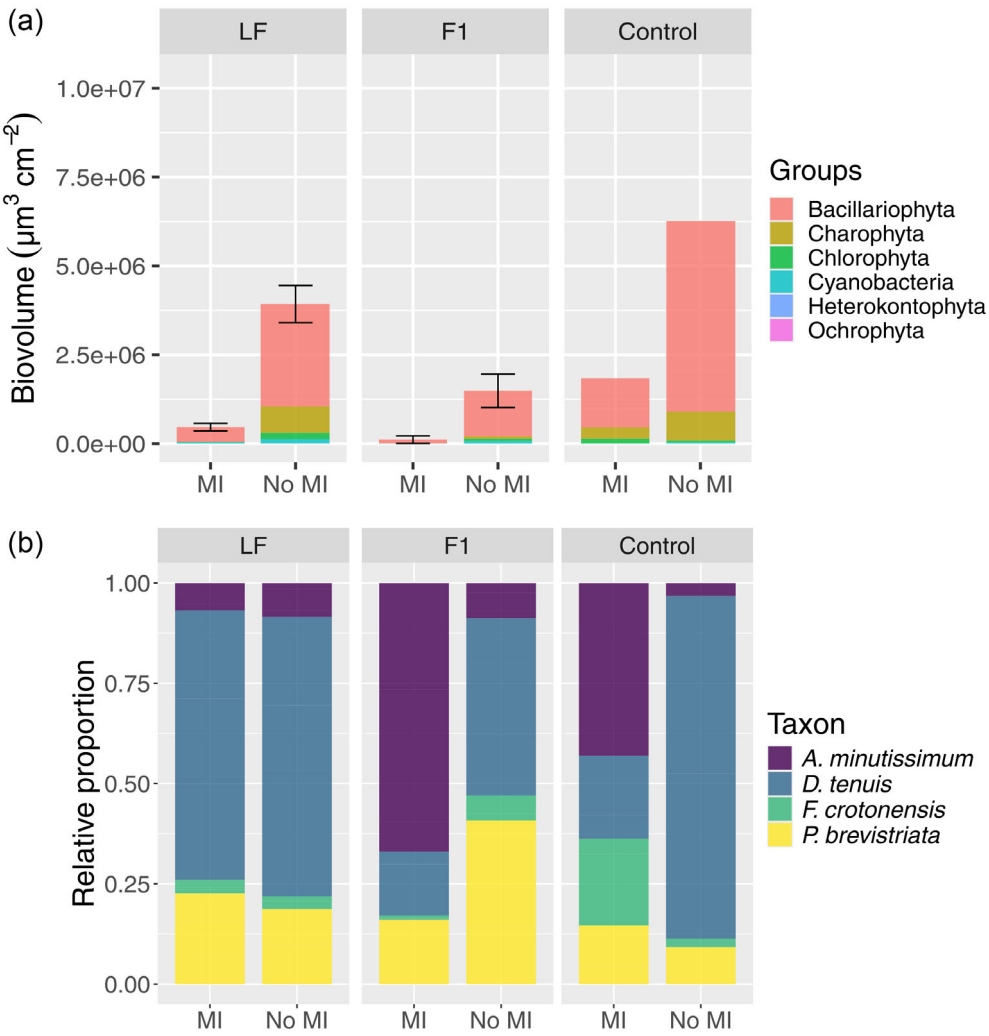

Fig. 3. (**a**) Mean biovolume of different algal groups (error bars represent standard error among mesocosms, $n = 3$ per treatment) and (**b**) relative proportions of the four major Bacillariophyta taxa, expressed as percentages of total Bacillariophyta biovolume, at low flow (LF) and during a flushing event (F1), with macroinvertebrates (MI) and without macroinvertebrates (No MI). Control mesocosms ($n = 1$ each) are shown for descriptive purposes only.

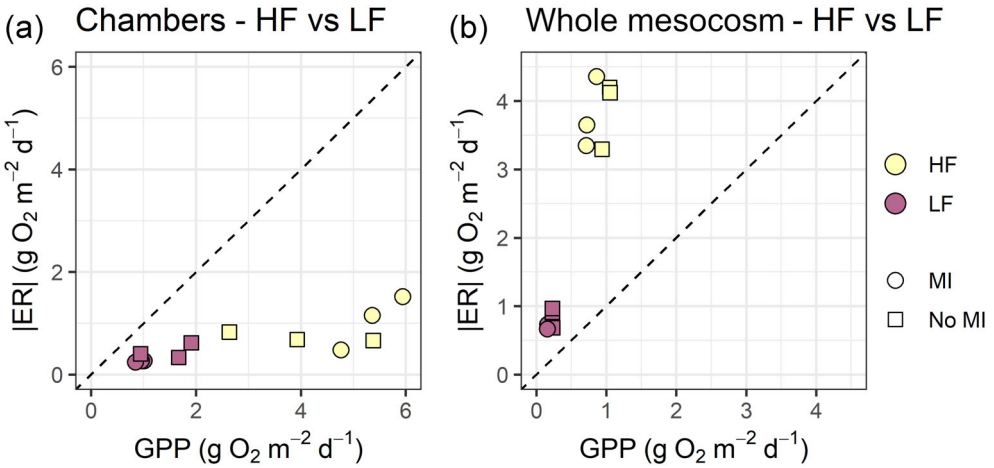

Fig. 4. Relationship between gross primary production (GPP) and ecosystem respiration (|ER|) under high flow (HF, red) and low flow (LF, blue) at the (**a**) chamber and (**b**) whole-mesocosm scales. Circles represent treatments with macroinvertebrates (MI) and squares represent treatments without macroinvertebrates (No MI). Each point represents a mesocosm-level mean ($n = 3$ per treatment). The dashed line indicates metabolic balance (GPP = |ER|); points below the line are net autotrophic and those above the line are net heterotrophic.

metabolic balance (Fig. 4b). Detailed statistical comparisons of GPP, ER, and NEP, including estimated marginal means, 95% CIs, and pairwise contrasts, are provided in Supporting Information Fig. S4 and Table S3. These analyses confirm that HF chambers had significantly higher NEP than LF chambers, whereas HF mesocosms were significantly more heterotrophic than LF mesocosms.

Flushing events

GPP responded strongly to flushing at the chamber scale, particularly in the absence of macroinvertebrates (No MI; Fig. 5a; Supporting Information Table S4). GPP increased from 1.47 g O_2 m^{-2} d^{-1} at LF (95% CI: 0.94–2.15) to 2.72 at F1 (+84%; $p = 0.033$ vs. LF) and peaked at 4.06 at F2 (+176%; $p = 0.002$). After the third flush, GPP decreased to 2.09 (+42% relative to LF; this difference was not statistically significant, $p = 0.173$), indicating a return toward initial values. In contrast, in chambers with macroinvertebrates (MI), GPP remained consistently lower, ranging from 0.94 at LF to 1.53 at F2, with no significant fluctuations across events.

ER remained relatively stable across treatments at the chamber scale (Fig. 5b; Supporting Information Table S4). In the absence of macroinvertebrates, ER values ranged between −0.45 and −0.17 g O_2 m^{-2} d^{-1}, with no significant differences across events (all $p > 0.05$). With macroinvertebrates, ER was also low and stable up to F2 (−0.26 to −0.14) but dropped sharply at F3 to −1.47 (relative to LF, $p = 0.04$).

NEP largely reflected GPP patterns at the chamber scale, with pronounced but statistically non-significant responses to flushing (Fig. 5c; Supporting Information Table S4). Without macroinvertebrates, NEP increased from 1.02 at LF to 2.44 at F1 (+139%) and peaked at 3.77 at F2 (+269%), although neither change was statistically significant ($p = 0.297$ and $p = 0.162$, respectively). After the third flush, NEP decreased to 1.86 (+82% relative to LF; $p = 0.334$), converging toward baseline. With macroinvertebrates, NEP rose more modestly, from 0.68 at LF to 1.38 at F2 (+103%; $p = 0.783$), and then turned negative at F3 (−0.39, a 157% decrease; $p = 0.248$).

At the whole-mesocosm scale, GPP increased consistently with flushing, regardless of macroinvertebrate presence. With macroinvertebrates, GPP rose from 0.17 g O_2 m^{-2} d^{-1} at LF (95% CI: 0.13–0.21) to 0.26 at F1 (+57%; $p < 0.001$) and 0.32 at F2 (+90%; $p < 0.001$). Without macroinvertebrates, values were higher overall and increased from 0.23 at LF to 0.39 at F1 (+68%; $p < 0.001$), remaining at 0.38 at F2 (+66%; $p < 0.001$) (Fig. 6a; Supporting Information Table S4). Although the dataset ended shortly after the third flushing event and we lacked sufficient data to model whole-mesocosm metabolism beyond F2, GPP (and consequently NEP) in mesocosms without macroinvertebrates already tended to plateau after the second flush, suggesting diminishing gains relative to the first event.

ER and NEP both shifted toward reduced heterotrophy with increasing flushing, especially in mesocosms without macroinvertebrates. ER became less negative with increasing flushing indicating a reduction in respiration magnitude. With macroinvertebrates, ER shifted from −0.70 at LF to −0.63 at F1 (+11%; $p = 0.15$) and −0.53 at F2 (+25%; $p = 0.005$). Without macroinvertebrates, ER showed a similar pattern, changing from −0.85 at LF to −0.60 at F1 (+30%; $p < 0.001$) and further to −0.50 at F2 (+41%; $p < 0.001$) (Fig. 6b; Supporting Information Table S4). NEP followed the trajectory of GPP. With macroinvertebrates, NEP increased (became less negative) from −0.53 at LF to −0.36 at F1 (+32%; $p = 0.005$) and −0.21 at F2 (+61%; $p < 0.001$). Without macroinvertebrates, NEP rose (became less negative) from

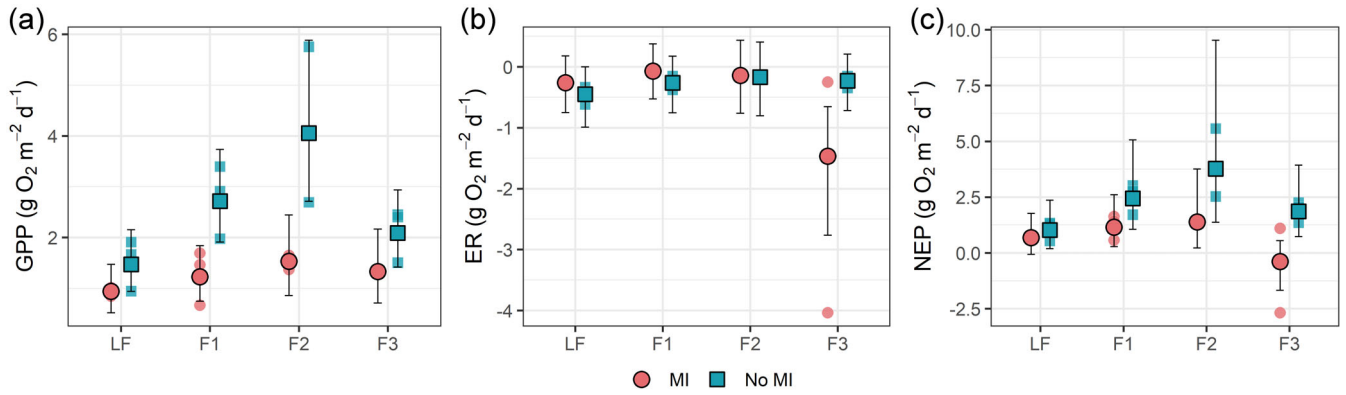

Fig. 5. Gross primary production (GPP), ecosystem respiration (ER), and net ecosystem production (NEP) (g O_2 m^{-2} d^{-1}) from chamber-scale measurements under different flow velocity treatments. Red circles represent mesocosms with macroinvertebrates (MI) and blue squares represent mesocosms without macroinvertebrates (No MI). Flow treatments include Low Flow (LF) and three flushing events of increasing frequency (F1, F2, F3). Symbols indicate mean values and error bars represent 95% confidence intervals of the mixed-effects model estimates from the chamber measurements ($n = 3$ per treatment).

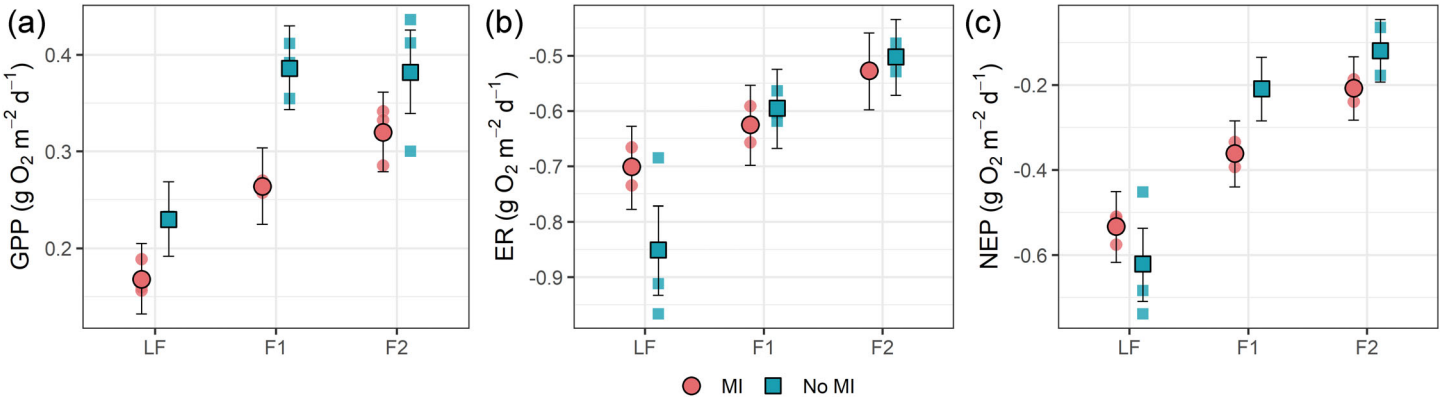

Fig. 6. Gross primary production (GPP), ecosystem respiration (ER), and net ecosystem production (NEP) (g O_2 m^{-2} d^{-1}) from whole-mesocosm measurements under different flow treatments. Red circles represent mesocosms with macroinvertebrates (MI) and blue squares represent mesocosms without macroinvertebrates (No MI). Flow treatments include low flow (LF) and two flushing events of increasing frequency (F1, F2). Symbols indicate mean values and error bars represent 95% confidence intervals of the mixed-effects model estimates at the whole-mesocosm scale ($n = 3$ per treatment).

−0.62 at LF to −0.21 at F1 (+66%; $p < 0.001$) and −0.12 at F2 (+81%; $p < 0.001$) (Fig. 6c, Supporting Information Table S4).

Discussion

Interactions among flow velocity, macroinvertebrates, and flushing events jointly shaped the structure and metabolism of periphyton communities. Gradual flow changes influenced ecosystem productivity, but the direction of responses depended on the compartment considered. At the chamber scale, which isolated periphyton activity, LF reduced autotrophic production, whereas at the whole-mesocosm scale, integrating the whole system, LF reduced both autotrophic and heterotrophic processes. Flushing events consistently altered metabolism, stimulating GPP and NEP during the first events but destabilizing the ecosystem when disturbance frequency increased, as responses peaked and then declined. When macroinvertebrates were present, the overall rates were lower but more stable across events, showing that their activity reduced fluctuations and helped stabilize metabolism and biomass against repeated flushing.

Algal biomass and composition

In the absence of macroinvertebrates, algal biovolume remained stable across flow treatments, while the presence of macroinvertebrates reduced algal biovolume under both high- and low-flow treatments. However, the magnitude of the effect was flow-dependent: algal biovolume decreased by ~ 70% at LF compared to only a modest reduction at HF (Fig. 2a). This pattern likely reflects reduced grazing efficiency under high-flow conditions, where stronger hydrodynamic forces constrain attachment and feeding (Rempel et al. 2000), resulting in greater algal accumulation. However, sufficiently high velocities can also scour periphyton, a threshold not

reached under our experimental conditions. This interaction between flow velocity and grazing is consistent with earlier studies showing that HF disrupts grazing by limiting attachment, whereas LF enables stable feeding and intensifies top-down control on periphyton biomass (Poff and Ward 1989). Consistently, the observed increase in *Gammarus* spp. biomass during the experiment indicates that macroinvertebrates exerted sustained grazing pressure, contributing to the reduction in periphyton biomass.

Macroinvertebrates influenced periphyton composition at both the group and species levels. Under LF without macroinvertebrates, Zygnematales (mainly *Mougeotia* spp.) increased markedly (+89.1%), while Cyanobacteria declined (−61.7%), shifting dominance from Cyanobacteria at HF to Chlorophyta at LF. With macroinvertebrates, such shifts were absent, suggesting that grazing buffered group-level changes. In contrast, within Bacillariophyta (the dominant algal group across all treatments), compositional differences were comparatively modest (Fig. 2b). In control mesocosms with macroinvertebrates, *Achnanthidium minutissimum* and *Fragilaria crotonensis* prevailed (32% and 35% of Bacillariophyta biovolume, respectively), whereas *Diatoma tenuis* predominated in the absence of macroinvertebrates under LF. These results indicate that macroinvertebrates altered periphyton primarily at the group level, while species-level responses within Bacillariophyta were smaller and more context-dependent.

Flushing events, in contrast to gradual flow reductions, introduced an additional stress that altered periphyton composition regardless of grazer presence. In macroinvertebrate mesocosms, *A. minutissimum* became proportionally more dominant after the first flush, while *D. tenuis* declined. In treatments without macroinvertebrates, Zygnematales (*Mougeotia* spp.) declined sharply after flushing, highlighting their vulnerability in the absence of grazing. Overall, flushing shifted community structure across both treatments, consistent with the subsidy–stress framework (Biggs et al. 1998), where intermediate disturbances may sustain biomass but repeated events destabilize periphyton communities.

Finally, control mesocosms ($n = 1$ each) provided qualitative evidence of successional changes: pioneer taxa such as *A. minutissimum* were initially dominant and later replaced by taxa typical of more mature periphyton assemblages (Sekar et al. 2004). While not included in statistical tests, these controls suggest that part of the observed variation reflects natural successional trajectories.

Metabolic responses to flow changes

Our results confirm that flow variability alters ecosystem metabolism, consistent with previous studies (Uehlinger et al. 2003; Bernhardt et al. 2022; O'Donnell and Hotchkiss 2022). The direction and magnitude of these responses depended on the biotic compartments included in the metabolic estimates. At the chamber scale, LF reduced periphyton productivity, as reflected in lower DO dynamics, consistent with reduced photosynthetic activity under diminished mixing and resource delivery (Stevenson et al. 1996; Peipoch et al. 2016). In contrast, whole-mesocosm measurements revealed that LF reduced both GPP and ER. This whole-system signal integrates contributions from periphyton, suspended organic matter, and sediments, and suggests that reduced flow simultaneously suppressed autotrophic and heterotrophic activity, likely by limiting resource supply and sediment resuspension. These differences highlight that chamber and mesocosm estimates capture distinct processes and stress the need to integrate multiple scales of observation. High flow had the opposite effect: it increased ER, consistent with increased turbidity, the remobilization of organic matter, and the stimulation of microbially driven respiration. Previous studies confirm that even small sediment movements can alter oxygen penetration, vertical water fluxes, and microbial activity (Mendoza-Lera and Mutz 2013; Scheidweiler et al. 2021; Risse-Buhl et al. 2023). This pattern indicates that flow impacts extend well beyond the periphyton layer and are strongly mediated by near-bed dynamics (Cardinale et al. 2002; Battin et al. 2008).

Flushing events added a temporal dimension. At the chamber scale, initial flushes stimulated GPP more than ER, increasing NEP, but repeated flushing progressively suppressed NEP, particularly after the third event, when periphyton structure was likely compromised. At the whole-mesocosm scale, flushing also increased both GPP and ER, and NEP rose after the first two events, but values remained negative, reflecting a whole-system tendency toward heterotrophy. Our findings indicate that while moderate disturbances can allow some degree of metabolic adjustment, increasing disturbance frequency destabilizes metabolic balance and shifts systems toward heterotrophy. Consistent with previous studies (Uehlinger 2000, 2006; Shabarova et al. 2021), frequent flushing events appear to exceed the functional recovery capacity of stream periphyton, reducing both resistance (the ability to maintain function) and resilience (the ability to recover after disturbance). Increasing disturbance frequency, as projected under ongoing hydrological variability, may thus reduce autotrophic function and destabilize stream metabolism, with implications for carbon cycling.

Macroinvertebrates as stabilizers

The macroinvertebrate assemblage not only reduced algal biomass but also stabilized metabolic responses to flow variation. While their presence lowered overall periphyton biovolume, herbivorous activity likely prevented excessive biomass accumulation (Hillebrand 2009), buffering the system against drastic shifts in GPP and NEP. At the same time, nutrient cycling may have been accelerated (Guasch et al. 2016), enhancing metabolic flexibility and contributing to higher NEP in control mesocosms with macroinvertebrates compared to mesocosms without them. By promoting turnover of periphyton biomass, the macroinvertebrate assemblage helped prevent extreme fluctuations in productivity and respiration following flushing events. They also mediated resilience

indirectly through their influence on community composition and trophic interactions. Previous studies have shown that metabolic responses to HFs vary depending on ecosystem characteristics (O'Donnell and Hotchkiss 2022), and our results suggest that macroinvertebrate assemblages play a central role in this regulation by shaping periphyton structure and function (Cibils-Martina et al. 2019). While physical factors such as substrate stability and disturbance intensity determine the baseline resistance and resilience of stream metabolism (Uehlinger et al. 2000; Uehlinger 2006), macroinvertebrate assemblages act as an additional stabilizing force, enhancing nutrient turnover and moderating the destabilizing effects of repeated disturbances. The interplay between macroinvertebrate activity, nutrient dynamics, and microbial processes remains complex, however, as heterotrophic bacteria may offset some of the carbon fixation benefits of increased nutrient cycling. Future research should therefore explore how macroinvertebrate activity, microbial dynamics, and flow disturbances interact to shape metabolic resistance and resilience in freshwater ecosystems facing more frequent and intense hydrological variability.

Our study demonstrates that flow variability interacts with community composition to shape stream metabolism, with consequences for riverine carbon cycling. These results emphasize the joint roles of hydrological dynamics and macroinvertebrate presence in regulating how energy and carbon are processed in running waters. By showing that the metabolic outcomes of flow disturbances depend on the presence of a macroinvertebrate assemblage, our findings suggest that reductions in consumer biomass could intensify the metabolic impacts of altered flow regimes. More broadly, they highlight the interplay between physical drivers and biological regulation in structuring the functional and structural characteristics of aquatic ecosystems. As hydrological variability increases under climate change, considering both flow dynamics and community composition will be important for advancing predictions of riverine carbon budgets.

Author Contributions

Flavia Tromboni, Alain Maasri, and Susana Bernal: Conceptualization. Flavia Tromboni, Silvia Mohr, Alain Maasri, and Carolina Jativa: Methodology, investigation. Carina Seitz and Marco Cantonati: Taxonomic analysis (periphyton). Alain Maasri: Taxonomic analysis (macroinvertebrates). Flavia Tromboni, Giulia Grandi, Enrico Bertuzzo, and Susana Bernal: Metabolism modeling. Carolina Jativa, Flavia Tromboni, and Anna Lupon: Formal analysis, statistics. Flavia Tromboni, Hans-Peter Grossart, Sonja C. Jähnig, Andreas Lorke, and Clara Mendoza-Lera: Funding acquisition. All authors: Data curation, writing—review and editing. Flavia Tromboni: Writing—original draft, project administration.

Acknowledgments

The project was supported through Transnational Access funds by the EU Project AQUACOSM, EU H2020-INFRAIA (Project No. 731065). The staff of the German Federal Environment Agency in preparation of the mesocosms for the project are greatly acknowledged. Flavia Tromboni was granted a Leibniz Institute of Freshwater Ecology and Inland Fisheries (IGB) visiting postdoctoral scholarship while conducting the experiments and received additional funding for this work from the European Union's Horizon 2020 research and innovation program under the Marie Skłodowska-Curie Grant Agreement No. 101105996. Carolina Jativa's work was supported by the FPU21/03523 from MICIU/AEI/10.13039/501100011033 and FSE+. Susana Bernal and Anna Lupon's work was supported by the projects EVASIONA (PID2021-122817-NB-100), RIPAMED (CNS2023-144737), OXIT (PID2024-158111NB-C21), INHOT (CNS2022-135690), and FLUPRINT (EUR2023-143456), funded by MICIU/AEI/10.13039/501100011033 and NextGenerationEU/PRTR. Sonja C. Jähnig considers this work a contribution to the Collaborative Research Centre 1439 RESIST (CRC 1439/2, grant number 426547801 funded by the Deutsche Forschungsgemeinschaft (DFG)). Clara Mendoza-Lera was funded by the Deutsche Forschungsgemeinschaft (DFG), under the project FlowReSeT (ME 5498/2-1). Open Access funding enabled and organized by Projekt DEAL.

Conflicts of Interest

None declared.

Data Availability Statement

The datasets generated and/or analyzed during the current study and code are publicly available: https://figshare.com/s/2c48feb905a24168ee3d; https://figshare.com/s/d4d7c9e88ea8635c46f1; https://figshare.com/s/ddb23fd1253cb6e1ce7f.

References

APHA. 2012. Standard Methods for the Examination of Water and Wastewater, edited by E. W. Rice, R. B. Baird, A. D. Eaton, and L. S. Clesceri, 22nd ed. American Public Health Association (APHA), American Water Works Association (AWWA) and Water Environment Federation (WEF).

Arsenault, E. R., J. H. Thorp, M. J. Polito, et al. 2022. "Intercontinental Analysis of Temperate Steppe Stream Food Webs Reveals Consistent Autochthonous Support of Fishes." *Ecology Letters* 25: 2624–2636. https://doi.org/10.1111/ele.14113.

Battin, T. J., K. Besemer, M. M. Bengtsson, A. M. Romani, and A. I. Packmann. 2016. "The Ecology and Biogeochemistry of Stream Biofilms." *Nature Reviews*

Microbiology 14: 251–263. https://doi.org/10.1038/nrmicro.2016.15.

Battin, T. J., L. A. Kaplan, S. Findlay, et al. 2008. "Biophysical Controls on Organic Carbon Fluxes in Fluvial Networks." *Nature Geoscience* 1: 95–100. https://doi.org/10.1038/ngeo101.

Battin, T. J., R. Lauerwald, E. S. Bernhardt, et al. 2023. "River Ecosystem Metabolism and Carbon Biogeochemistry in a Changing World." *Nature* 613: 449–459. https://doi.org/10.1038/s41586-022-05500-8.

Bellinger, E. G., and D. C. Sigee. 2015. Freshwater Algae: Identification, Enumeration and Use as Bioindicators. Wiley-Blackwell.

Bernhardt, E. S., P. Savoy, M. J. Vlah, et al. 2022. "Light and Flow Regimes Regulate the Metabolism of Rivers." *Proceedings of the National Academy of Sciences of the United States of America* 119: e2121976119. https://doi.org/10.1073/pnas.2121976119.

Biggs, B. J. F., D. G. Goring, and V. I. Nikora. 1998. "Subsidy and Stress Responses of Stream Periphyton to Gradients in Water Velocity as a Function of Community Growth Form." *Journal of Phycology* 34: 598–607. https://doi.org/10.1046/j.1529-8817.1998.340598.x.

Cardinale, B. J., M. A. Palmer, C. M. Swan, S. Brooks, and N. L. Poff. 2002. "The Influence of Substrate Heterogeneity on Biofilm Metabolism in a Stream Ecosystem." *Ecology* 83: 412–422. https://doi.org/10.1890/0012-9658(2002)083[0412:TIOSHO]2.0.CO;2.

Cibils-Martina, L., J. A. Márquez, E. N. Gari, R. Albariño, and R. E. Príncipe. 2019. "Disentangling Grazing and Light Controls on Algal Communities in Grassland and Afforested Streams." *Ecological Research* 34: 136–149. https://doi.org/10.1111/1440-1703.1014.

Cunha, D. G. F., N. R. Finkler, M. C. Calijuri, T. P. Covino, F. Tromboni, and W. K. Dodds. 2018. "Nutrient Uptake in a Simplified Stream Channel: Experimental Manipulation of Hydraulic Residence Time and Transient Storage." *Ecohydrology* 11: e2012. https://doi.org/10.1002/eco.2012.

Grace, M. R., and S. J. Imberger. 2006. Stream Metabolism: Performing & Interpreting Measurements. Water Studies Centre, Monash University, Murray Darling Basin Commission, and NSW Department of Environment and Climate Change.

Guasch, H., M. Ricart, J. López-Doval, et al. 2016. "Influence of Grazing on Triclosan Toxicity to Stream Periphyton." *Freshwater Biology* 61: 2002–2012. https://doi.org/10.1111/fwb.12797.

Guiry, M. D., and G. M. Guiry. 2023. "AlgaeBase." World-Wide Electronic Publication, National University of Ireland, Galway. Accessed December 26, 2023. http://www.algaebase.org.

Hall, R. O., and E. R. Hotchkiss. 2017. "Chapter 34—Stream Metabolism." In Methods in Stream Ecology, edited by G. A. Lamberti and F. R. Hauer, 3rd ed., 219–233. Academic Press.

Hillebrand, H. 2009. "Meta-Analysis of Grazer Control of Periphyton Biomass across Aquatic Ecosystems." *Journal of Phycology* 45: 798–806. https://doi.org/10.1111/j.1529-8817.2009.00702.x.

IPCC. 2022. "Climate Change 2022: Impacts, Adaptation and Vulnerability." In Contribution of Working Group II to the Sixth Assessment Report of the Intergovernmental Panel on Climate Change, edited by H.-O. Pörtner, D. C. Roberts, M. Tignor, et al. Cambridge University Press.

Jativa, C., A. Lupon, E. Lannergård, et al. 2025. "Breathing Storms: Enhanced Ecosystem Respiration During Storms in a Heterotrophic Headwater Stream." *EGUsphere* 22: 6411–6425. https://doi.org/10.5194/bg-22-6411-2025.

Kirk, J. T. O. 1994. "Light and Photosynthesis in Aquatic Ecosystems. 2nd Edition, xvi, 509p. Cambridge University Press." *Journal of the Marine Biological Association of the United Kingdom*. 74, no. 4: 987–987. https://doi.org/10.1017/S0025315400090366.

Lamberti, G. A., and V. H. Resh. 1983. "Stream Periphyton and Insect Herbivores: An Experimental Study of Grazing by a Caddisfly Population." *Ecology* 64: 1124–1135. https://doi.org/10.2307/1937823.

Maasri, A., S. C. Jähnig, M. C. Adamescu, et al. 2022. "A Global Agenda for Advancing Freshwater Biodiversity Research." *Ecology Letters* 25: 255–263. https://doi.org/10.1111/ele.13931.

Mendoza-Lera, C., and M. Mutz. 2013. "Microbial Activity and Sediment Disturbance Modulate the Vertical Water Flux in Sandy Sediments." *Freshwater Science* 32: 26–38. https://doi.org/10.1899/11-165.1.

Moulton, T. P., C. Lourenço-Amorim, C. Y. Sasada-Sato, V. Neres-Lima, and E. Zandonà. 2015. "Dynamics of Algal Production and Ephemeropteran Grazing of Periphyton in a Tropical Stream." *International Review of Hydrobiology* 100: 61–68. https://doi.org/10.1002/iroh.201401769.

Mulholland, P. J., C. S. Fellows, J. L. Tank, et al. 2001. "Inter-Biome Comparison of Factors Controlling Stream Metabolism." *Freshwater Biology* 46: 1503–1517. https://doi.org/10.1046/j.1365-2427.2001.00773.x.

Noble, P. J., C. Seitz, S. S. Lee, K. M. Manoylov, and S. Chandra. 2023. "Characterization of Algal Community Composition and Structure from the Nearshore Environment, Lake Tahoe (United States)." *Frontiers in Ecology and Evolution* 10: 10. https://doi.org/10.3389/fevo.2022.1053499.

O'Donnell, B., and E. R. Hotchkiss. 2022. "Resistance and Resilience of Stream Metabolism to High Flow Disturbances." *Biogeosciences* 19: 1111–1134. https://doi.org/10.5194/bg-19-1111-2022.

Odum, H. T. 1956. "Primary Production in Flowing Waters." *Limnology and Oceanography* 1: 102–117. http://10.4319/lo.1956.1.2.0102.

Palmer, C. M., and T. E. A. Maloney. 1954. New Counting Slide for Nanoplankton. American Society of Limnology and Oceanography Special Publication.

Palmer, M., and A. Ruhi. 2019. "Linkages Between Flow Regime, Biota, and Ecosystem Processes: Implications for River Restoration." *Science* 365: eaaw2087. https://doi.org/10.1126/science.aaw2087.

Peipoch, M., E. Gacia, E. Bastias, et al. 2016. "Small-Scale Heterogeneity of Microbial N Uptake in Streams and its Implications at the Ecosystem Level." *Ecology* 97: 1329–1344. https://doi.org/10.1890/15-1210.1.

Poff, N. L., J. D. Allan, M. B. Bain, et al. 1997. "The Natural Flow Regime. A Paradigm for River Conservation and Restoration." *Bioscience* 47: 769–784. https://doi.org/10.2307/1313099.

Poff, N. L., and a J V. Ward. 1989. "Implications of Streamflow Variability and Predictability for Lotic Community Structure: A Regional Analysis of Streamflow Patterns." *Canadian Journal of Fisheries and Aquatic Sciences* 46: 1805–1818. https://doi.org/10.1139/f89-228.

R Core Team. 2022. R: A Language and Environment for Statistical Computing. R.F.F.S. Computing.

Rempel, L. L., J. S. Richardson, and M. C. Healey. 2000. "Macroinvertebrate Community Structure along Gradients of Hydraulic and Sedimentary Conditions in a Large Gravel-Bed River." *Freshwater Biology* 45: 57–73. https://doi.org/10.1046/j.1365-2427.2000.00617.x.

Rimet, F., and J. C. Druart. 2018. "A Trait Database for Phytoplankton of Temperate Lakes." *Annales de Limnologie - International Journal of Limnology* 54: 18. https://doi.org/10.1051/limn/2018009.

Risse-Buhl, U., S. Arnon, E. Bar-Zeev, et al. 2023. "Streambed Migration Frequency Drives Ecology and Biogeochemistry Across Spatial Scales." *WIREs Water* 10: e1632. https://doi.org/10.1002/wat2.1632.

Rüegg, J., J. D. Brant, D. M. Larson, M. T. Trentman, and W. K. Dodds. 2015. "A Portable, Modular, Self-Contained Recirculating Chamber to Measure Benthic Processes Under Controlled Water Velocity." *Freshwater Science* 34: 831–844. https://doi.org/10.1086/682328.

Rüegg, J., C. C. Conn, E. P. Anderson, et al. 2021. "Thinking Like a Consumer: Linking Aquatic Basal Metabolism and Consumer Dynamics." *Limnology and Oceanography Letters* 6: 1–17. https://doi.org/10.1002/lol2.10172.

Sabater, S., A. Freixa, L. Jiménez, et al. 2023. "Extreme Weather Events Threaten Biodiversity and Functions of River Ecosystems: Evidence from a Meta-Analysis." *Biological Reviews* 98: 450–461. https://doi.org/10.1111/brv.12914.

Sayer, C. A., E. Fernando, R. R. Jimenez, et al. 2025. "One-Quarter of Freshwater Fauna Threatened with Extinction." *Nature* 638: 138–145. https://doi.org/10.1038/s41586-024-08375-z.

Scheidweiler, D., C. Mendoza-Lera, M. Mutz, and U. Risse-Buhl. 2021. "Overlooked Implication of Sediment Transport at Low Flow: Migrating Ripples Modulate Streambed Phototrophic and Heterotrophic Microbial Activity." *Water Resources Research* 57: e2020WR027988. https://doi.org/10.1029/2020WR027988.

Sekar, R., V. P. Venugopalan, K. Nandakumar, K. V. K. Nair, and V. N. R. Rao. 2004. "Early Stages of Biofilm Succession in a Lentic Freshwater Environment." *Hydrobiologia* 512: 97–108. https://doi.org/10.1023/B:HYDR.0000020314.69538.2c.

Serieyssol, K. 2012. Diatoms of Europe: Diatoms of the European Inland Waters and Comparable Habitats. Vol. 1. Koeltz Botanical Books.

Shabarova, T., M. M. Salcher, P. Porcal, et al. 2021. "Recovery of Freshwater Microbial Communities after Extreme Rain Events Is Mediated by Cyclic Succession." *Nature Microbiology* 6: 479–488. https://doi.org/10.1038/s41564-020-00852-1.

Spaulding, S. A., M. G. Potapova, I. W. Bishop, et al. 2021. "Diatoms.org: Supporting Taxonomists, Connecting Communities." *Diatom Research* 36: 291–304. https://doi.org/10.1080/0269249X.2021.2006790.

Stach, T. L., A. Deep, I. Madge Pimentel, et al. 2024. "Complex Compositional and Cellular Response of River Sediment Microbiomes to Multiple Anthropogenic Stressors." bioRxiv. 2024.06.07.597903.

Steinman, A. D., P. J. Mulholland, and J. J. Beauchamp. 1995. "Effects of Biomass, Light, and Grazing on Phosphorus Cycling in Stream Periphyton Communities." *Journal of the North American Benthological Society* 14, no. 3: 371–381. https://doi.org/10.2307/1467203.

Stevenson, R. J., M. L. Bothwell, and R. L. Lowe. 1996. Algal Ecology: Freshwater Benthic Ecosystems. Academic Press.

Tachet, H., P. Richoux, M. Bournaud, and P. Usseglio-Polatera. 2010. Invertébrés d'eau douce: systématique, biologie, écologie. Vol. 15. CNRS Éditions.

ter Braak, C. J. F., and J. A. Vrugt. 2008. "Differential Evolution Markov Chain With Snooker Updater and Fewer Chains." *Statistics and Computing* 18: 435–446. https://doi.org/10.1007/s11222-008-9104-9.

Tromboni, F., W. K. Dodds, S. Chandra, S. R. Poulson, A. Pandey, and A. Schechner. 2020. "Respiration in Rivers Fractionates Stable Isotopes of Dissolved Oxygen; a Global Investigation on the Influences of Temperature and Flow." *Biogeochemistry* 147: 199–210. https://doi.org/10.1007/s10533-020-00636-z.

Tromboni, F., W. K. Dodds, V. Neres-Lima, E. Zandonà, and T. P. Moulton. 2017. "Heterogeneity and Scaling of Photosynthesis, Respiration, and Nitrogen Uptake in Three Atlantic Rainforest Streams." *Ecosphere* 8: e01959. https://doi.org/10.1002/ecs2.1959.

Tromboni, F., E. R. Hotchkiss, A. E. Schechner, W. K. Dodds, S. R. Poulson, and S. Chandra. 2022. "High Rates of Daytime River Metabolism Are an Underestimated Component of Carbon Cycling." *Communications Earth & Environment* 3: 270. https://doi.org/10.1038/s43247-022-00607-2.

Uehlinger, U. 2000. "Resistance and Resilience of Ecosystem Metabolism in a Flood-Prone River System." *Freshwater Biology* 45: 319–332. https://doi.org/10.1111/j.1365-2427.2000.00620.x.

Uehlinger, U. 2006. "Annual Cycle and Inter-Annual Variability of Gross Primary Production and Ecosystem Respiration in a Floodprone River During a 15-Year Period." *Freshwater Biology* 51: 938–950. https://doi.org/10.1111/j.1365-2427.2006.01551.x.

Uehlinger, U., B. Kawecka, and C. T. Robinson. 2003. "Effects of Experimental Floods on Periphyton and Stream Metabolism below a High Dam in the Swiss Alps (River Spöl)." *Aquatic Sciences* 65: 199–209. https://doi.org/10.1007/s00027-003-0664-7.

Uehlinger, U., C. König, and P. Reichert. 2000. "Variability of Photosynthesis-Irradiance Curves and Ecosystem Respiration in a Small River." *Freshwater Biology* 44: 493–507. https://doi.org/10.1046/j.1365-2427.2000.00602.x.

Weehr, J. D., R. G. Sheath, and J. P. Kociolek, eds. 2015. Freshwater Algae of North America: Ecology and Classification. 2nd ed. Academic Press.

Supporting Information

Additional Supporting Information may be found in the online version of this article.

Submitted 26 February 2025
Revised 29 September 2025
Accepted 24 November 2025